

ITC 1/54 Information Technology and Control Vol. 54 / No. 1/ 2025 pp. 135-146 DOI 10.5755/j01.itc.54.1.39368	Real-time Detection of Pipeline Weld Defects Based on Lightweight Neural Networks	
	Received 2024/11/04	Accepted after revision 2024/01/31
	HOW TO CITE: Yu, Z., Yu, H. (2025). Real-time Detection of Pipeline Weld Defects Based on Lightweight Neural Networks. <i>Information Technology and Control</i> , 54(1), 135-146. https://doi.org/10.5755/j01.itc.54.1.39368	

Real-time Detection of Pipeline Weld Defects Based on Lightweight Neural Networks

Zeyu Yu

Jingzhou Institute of Technology, China; e-mail: yuzeyu_jz@163.com

Huayun Yu

Yangtze University, China; e-mail: yhuayun88@sina.com

Corresponding author: yhuayun88@sina.com

In the field of pipeline weld defect detection, common object detection algorithms have high complexity and huge computational load, making it difficult to meet the real-time monitoring requirements of pipeline weld defects on pipeline production lines. To address this issue, this paper proposes a lightweight pipeline weld defect detection model YOLOv8n-BVS based on the YOLOv8n object detection framework. The model introduces the BRA module to improve the recognition ability of small defects. To further improve the accuracy of model recognition, a lightweight upsampling algorithm CARAFE is used in the feature fusion network to improve the quality and richness of fused features. Finally, the experimental results showed that the model parameters were 1.56M, which was only 51.6% of the baseline, while the average accuracy reached 87.9%, an improvement of 3.4% compared to the baseline. This verified that the YOLOv8n-BVS model met the requirements of online detection of pipeline weld defects while ensuring detection quality.

KEYWORDS: Lightweight neural network; Pipeline welds; Defect detection; Real-time recognition.

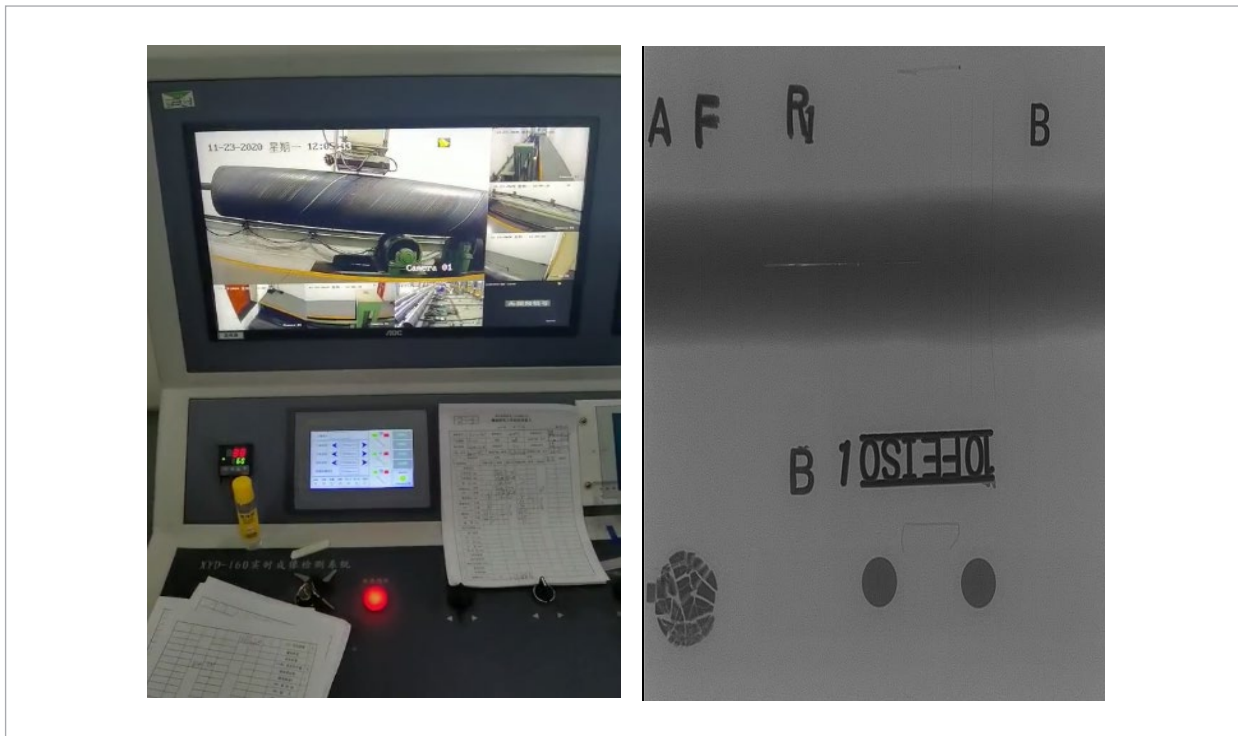
1. Introduction

Welding is the most important production method for oil and gas pipelines, and the quality of welds is an important factor in ensuring the safety of oil and gas pipelines. Detecting weld defects through X-ray is an important technical means to ensure weld quality. At

present, in this testing position, practitioners must observe the X-ray pipeline weld seam detection images returned on the assembly line in real-time, and judge defects based on their professional knowledge and experience. This method has high work intensity,

Figure 1

Job positions and inspection drawings for pipeline weld defect detection



strong subjectivity, and high responsibility, resulting in a sharp decrease in the number of relevant practitioners year by year. There is an urgent need for an intelligent defect detection method to alleviate work pressure [5, 11].

With the development of artificial intelligence technology, deep learning methods are widely used in industrial quality inspection. The research on pipeline weld defect detection using deep learning methods is gradually increasing. However, due to the large computational resources required for training and testing of deep neural network models, and the limited computing power of deploying terminal devices, it is difficult to achieve real-time and efficient recognition results. Moreover, the pipeline running speed on the pipeline weld defect detection pipeline is relatively fast. The industrial deployment of intelligent research results on pipeline defects has brought significant difficulties and challenges. Most existing research on pipeline weld seam defect recognition has not taken into account the capture of small defects in the detection image during pipeline travel, which can lead to

missed detections [15, 18]. Therefore, reducing model complexity and computational complexity as much as possible while ensuring detection accuracy is an important issue that needs to be addressed in this field. YOLO, as a classic stage object detection algorithm, has the advantages of high real-time performance, simplicity and efficiency, multi-scale detection, global contextual information utilization, and multitasking [7]. These characteristics make it perform well in fast object detection and real-time application scenarios. On the other hand, the large number of parameters and high computational cost of YOLO series models make it difficult to achieve industrial deployment of defect detection research results. Therefore, how to improve the YOLO series while ensuring high object detection performance is a hot research topic.

In the task of detecting defects in pipeline welds, the computing power of terminal detection equipment is often only a few GFLOPS levels, and the memory is less than 8GB. However, at present, YOLO-based object detection algorithms generally have a computing power of 40-150GFLOPS. Predicting a

640 x 640 image requires about 16GB of memory, which exceeds the processing capacity of terminal detection equipment. Without increasing computing resources, terminal detection devices cannot guarantee the stable operation of object detection models with large computational complexity [3, 12]. In addition, higher detection accuracy is needed to meet practical production needs, especially in identifying small defects such as pores and cracks.

2. Related Work

Defect detection is a highly promising application scenario for deep learning. Compared with traditional computer vision algorithms and statistical learning methods, deep learning defect recognition methods have higher detection accuracy and stronger robustness in complex backgrounds [1, 4]. Researchers are increasingly interested in using deep learning-based methods to detect defects in pipeline welds. Some studies have proposed hybrid methods that combine multiple deep-learning algorithms. For example, a feature pyramid network FPN model based on Faster RCNN was proposed to address defects of different sizes in welds, weak contrast, and wide boundary transitions in X-ray images, and a new visual attention mechanism SPAM (Squeeze and Position Attention Mechanism) was introduced [14]. Based on the idea of zero sample learning (ZSL), the semantic description of defect categories by experts is fully utilized to cross-integrate artificial semantic features with ultrasound detection signal features [9]. A study has focused on small defects in pipeline circumferential welds, using the Convolutional Block Attention Module (CBAM) to optimize the YOLOv5 network model structure and improve the detection network's attention preference for extracting small target defect signals [17]. The CBAM+YOLOv5 model improved the detection accuracy of MFL signals for pipeline circumferential welds from 89.33% to 98.11%, and correctly identified and classified the MFL signals of pipeline circumferential welds with a confidence level of 85%, with slight anomalies [16]. The current advanced deep learning-based object detection algorithms are difficult to deploy in some industrial production scenarios due to their overly complex models and large computational complexity, which are limited by the computing power of terminal detection de-

vices. To solve these problems, Chen et al. [2] proposed a lightweight architecture FNNet based on CNN for fabric defect detection. Compared with advanced lightweight architectures, FNNet has a faster training speed and computational resources are required. Xu et al. [18] designed a lightweight pipeline weld surface defect detection algorithm, using MobileNetV2 as the backbone network to construct a defect classification model, and introduced a CBAM dual channel attention module to improve the detection accuracy of the model while reducing its complexity. Wang et al. proposed a lightweight transmission line defect detection method based on coordinate attention. This method decouples the large convolution kernels in the network in both channel and space using YOLOv5, reducing the parameters of the convolution kernels and the computational complexity of convolution operations, achieving the lightweight of the network [15]. Kumar et al. designed GMANet as a bottleneck network based on the Ghost module and redesigned the feature fusion network to obtain a lightweight surface defect detection algorithm [8].

3. Methodology

This study focuses on addressing the limitations of computational power in online pipeline weld defect detection on terminal devices, where high computational complexity often hampers real-time performance. Using the YOLOv8n model as a baseline, we developed a pipeline weld defect detection model that balances detection accuracy and speed through three key improvements. First, to address the common issue of small defects being easily missed or misdiagnosed, we introduce the Bi-level Routing Attention (BRA) mechanism to enhance feature extraction. This improves the detection of small objects and boosts the overall performance of the YOLOv8n-based object detection model. Second, to reduce model complexity and the computational burden of traditional convolutions, we replace conventional convolution operations with the VanillaNet module in both the backbone and bottleneck networks. Finally, to further enhance detection performance, we incorporate the CARAFE module during the upsampling process. Traditional interpolation methods can blur or distort detailed features, but CARAFE preserves this information more effectively, allowing for more accurate

recovery of subtle features such as micropores and small cracks. This improves the model's ability to detect fine defects in pipeline welds.

3.1. Optimization of Small Defect Recognition Capability

Divide the input feature map $X \in \mathbb{R}^{H \times W \times C}$ of the obtained detection image into $S \times S$ non overlapping regions, so that each region contains HW/S^2 feature vectors. X is transformed into $X^r \in \mathbb{R}^{(S^2 \times HW/S^2) \times C}$ through reshaping operation, and linear mapping is obtained to obtain linear maps Q, K, V , as shown in public Equations (1)-(3):

$$Q = X^r W^q \quad (1)$$

$$K = X^r W^k \quad (2)$$

$$V = X^r W^v \quad (3)$$

Calculate the average values of regions Q and K separately to obtain $Q^r, K^r \in \mathbb{R}^{S^2 \times C}$, and then perform matrix multiplication on the obtained average values to obtain the adjacency matrix A^r of the affinity graph between regions, as shown in public Equation (4):

$$A^r = Q^r (W^r)^T \quad (4)$$

In the adjacency matrix A^r , each element represents the semantic correlation between two regions. A routing index matrix is generated through top-k operation to preserve the first k connections between each region and other regions. The result is shown in public Equation (5):

$$I^r = \text{topIndex}(A^r) \quad (5)$$

The i -th row of I^r contains the k most relevant indexes of the i -th region. Calculate the tensors V and K as shown in public Equations (6)-(7):

$$K^g = \text{gather}(K, I^r) \quad (6)$$

$$V^g = \text{gather}(V, I^r), \quad (7)$$

wherein, $K^g, V^g \in \mathbb{R}^{S^2 \times kHW/S^2 \times C}$ after obtaining the region to region routing index matrix I^r , for each Q in region i , it will focus on the key-values located in routing regions and concentrated on them. These regions are dispersed throughout the entire feature map by index $I^r_{(i,1)}, I^r_{(i,2)}, \dots, I^r_{(i,k)}$, and all K and V in these k regions are gathered, applying attention to K^g and V^g .

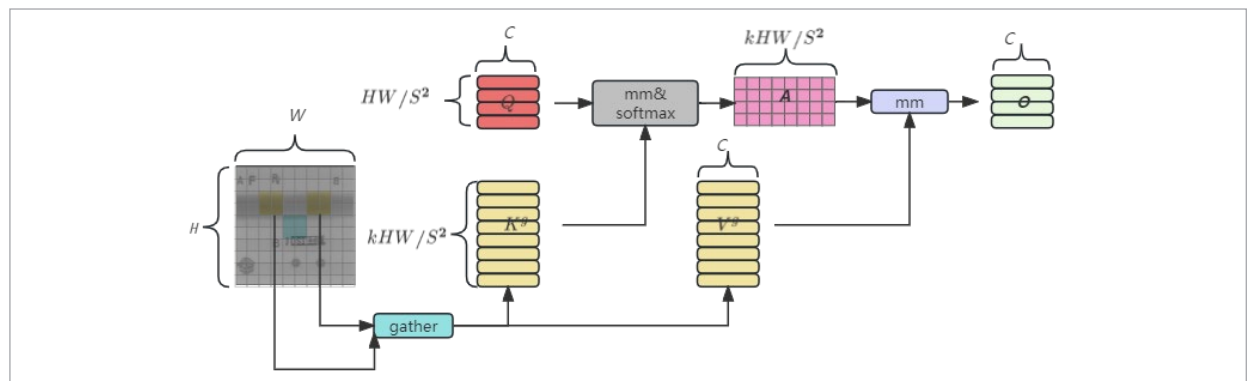
$$O = \text{Attention}(Q, K^g, V^g) + \text{LCE}(V), \quad (8)$$

where $\text{LCE}(V)$ is the local context enhancement term, function $\text{LCE}(V)$ parameterizes using deep convolution and sets the kernel size to 5.

The directed graph routing between regions enables the feature map to optimize the selection of related content in parts, not only enabling more accurate defect targets to be selected overall but also obtaining receptive field content more accurately in local areas. This means that the BRA mechanism based on double-layer routing has a more accurate receptive field selection ability [18, 20]. BRA is a dynamic sparse attention based on double-layer routing, which can achieve more flexible computation allocation and internal perception, making it have dynamic query-aware sparsity. The schematic diagram of its structure is shown in Figure 2.

Figure 2

The network structure of Bi-level routing attention



3.2. Research on Model Lightweight

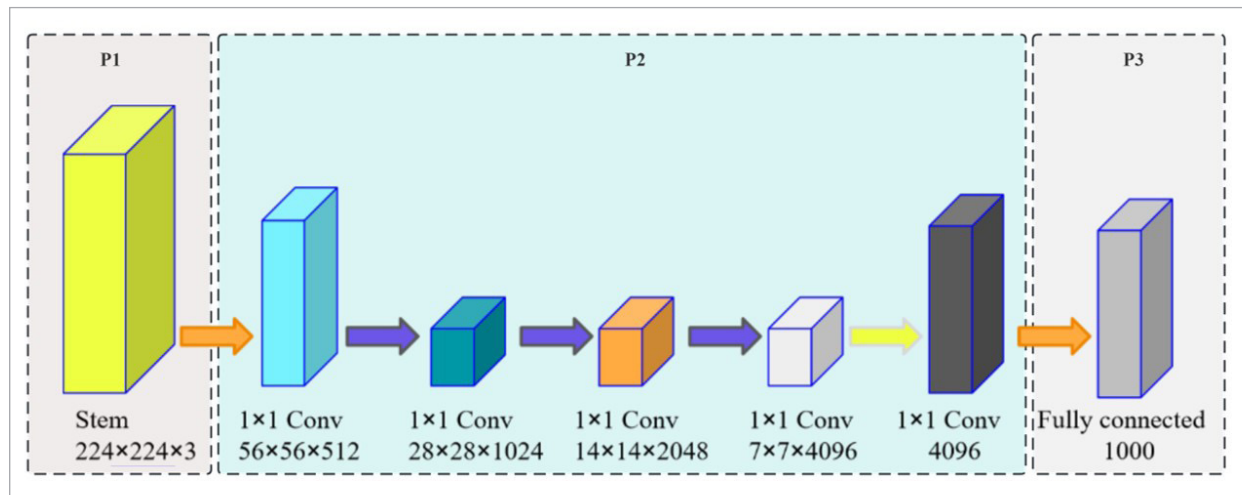
On the pipeline production line, where the average speed of pipeline operation reaches 0.15 m/s, real-time defect recognition poses a significant challenge. To address this, we replace the traditional convolutional operation in the YOLOv8n model's backbone with the lightweight VanillaNet module. Conventional convolution operations are computationally expensive, making them unsuitable for real-time pipeline defect detection. VanillaNet, a minimalist neural network developed by Huawei Noah and the University of Sydney, simplifies the convolution process by removing residual and attention modules, achieving strong performance across various computer vision tasks. The 13-layer VanillaNet model, for instance, reaches 83% accuracy on ImageNet, demonstrating that complex deep learning designs are not always necessary

for effective performance. By introducing VanillaNet in place of traditional convolutions, we retain strong feature aggregation performance while significantly improving the detection efficiency of the model.

As shown in Figure 3, the network consists of three stages. In the P1 stage, Stem converts the original 3-channel image into a feature map with C channels through downsampling. Then, in the P2 stage, a max pooling layer with a step size of 2 is used to adjust the size of the feature map and expand the number of channels to twice that of the previous layer. Finally, the classification results are output through the fully connected layer in the P3 stage. To preserve the feature information contained in the feature map and minimize computational costs, all convolutional layers use a 1×1 kernel, and BN is added to the end of each layer to simplify the training process of the network.

Figure 3

The network structure of VanillaNet



3.3. Model Performance Optimization

Pipeline weld seam detection images often suffer from high background noise, making it difficult for the model to distinguish useful defect information during the upsampling process. This results in poor-quality feature maps and excessive interference, ultimately affecting the model's detection accuracy. To address this issue and enhance the model's ability to express defect features, we introduce the lightweight CARAFE upsampling algorithm into the feature fusion

network of the YOLOv8n baseline model. Traditional upsampling methods typically neglect the semantic information in feature maps and have limited receptive fields, leading to suboptimal performance. CARAFE overcomes these limitations with its two key components: the upsampling kernel prediction module and the content-aware recombination module. The upsampling kernel prediction module generates an upsampling kernel that predicts the attention weights for each position, based on the mapping relationship of the downsampled feature map. This en-

sures that spatial details and contextual information are preserved during feature recombination. The content-aware recombination module further enhances the upsampling process by retaining as much spatial information as possible, improving the accuracy of object boundaries and defect detection. The specific process of upsampling is as follows: For the input feature map, $C \times H \times W$ with a size of X and an upsampling ratio of σ , a 1×1 convolution is used to compress its channel count to obtain a new feature map X' with a size of $C \times \sigma H \times \sigma W$. For any target position L of X' , there is a corresponding source position $l' = (i', j')$ on X , where $i = (i'/\sigma)$, $j = (j'/\sigma)$. If $N(X_p, k)$ is the $k \times k$ sub-domain of X centered on position l , then kernel pre-

diction module Ψ predicts a position kernel for each position based on the neighborhood of X_p , which l' can be represented as public Equation (9):

$$W(l') = \Psi(N(X_p, X_{encoder})). \quad (9)$$

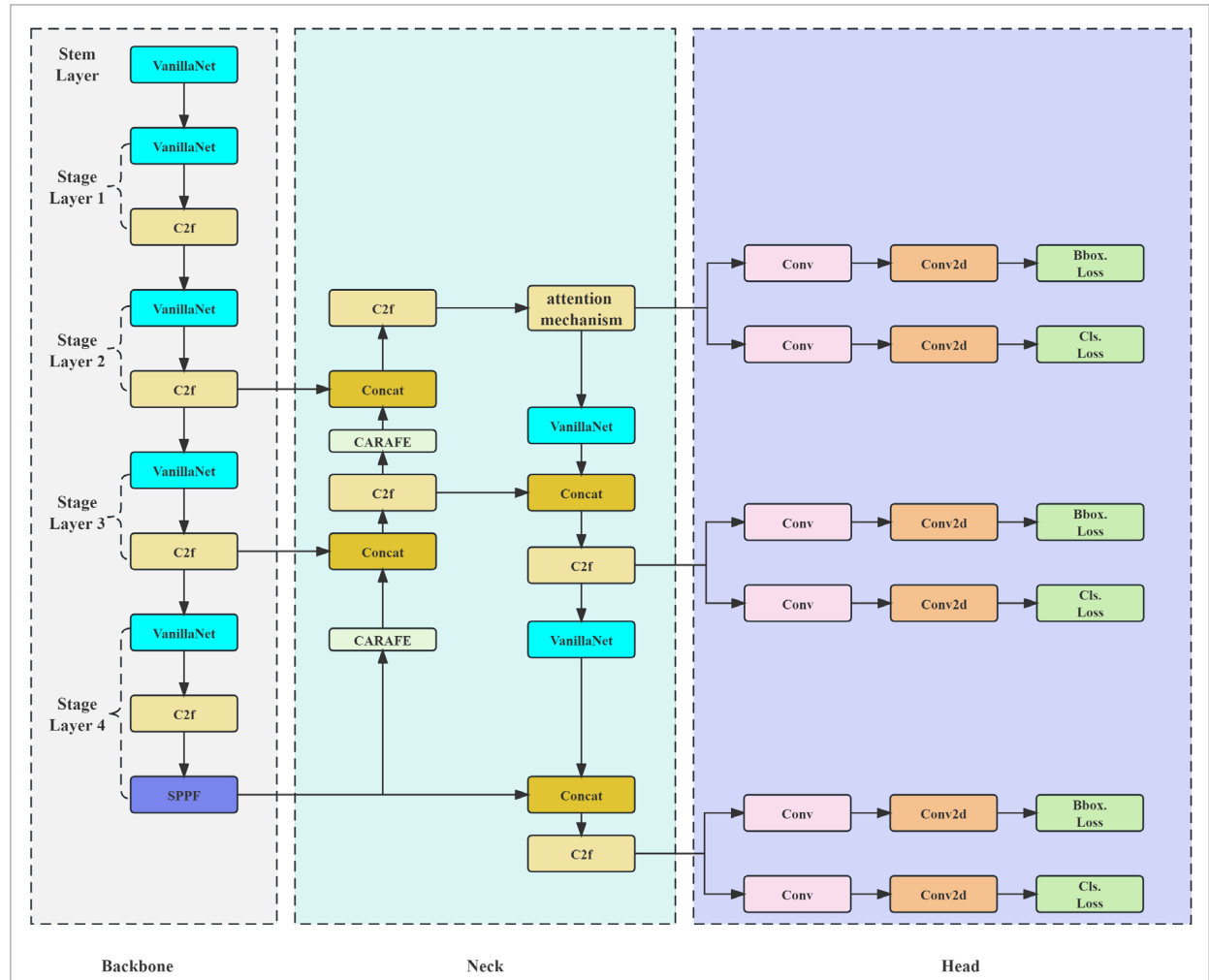
Recombine the features with the content perception restructuring module Φ , and recombine the neighborhood of X_l with the kernel $W(l')$ to obtain $X(l)'$ as shown in public Equation (10):

$$X_{l'} = \Phi(N(X_p, K_{up}), W_{l'}). \quad (10)$$

In summary, the YOLOv8n-BVS network structure proposed in this article is shown in Figure 4.

Figure 4

The network structure of YOLOv8n-BVS



4. Results and Discussion

4.1. Datasets and Evaluation Indicators

The data for this experiment comes from real X-ray inspection images of steel pipe manufacturing plants. Due to the strong professionalism of defect determination in X-ray inspection images, this study conducted a one-year special cooperation with data annotation engineers stationed in the steel pipe manufacturing plant to assist X-ray inspectors in standardizing and annotating X-ray inspection images of real pipeline weld defects, and constructing a professional and standardized defect annotation dataset. The common five types of pipeline weld defects are shown in Figure 5.

This research experiment used a single GPU (NVIDIA GeForce RTX 3080 16G) during the training phase, with an image input size of 640 * 640, an initial learning rate of 0.025, a Batchsize of 16, an SGD optimizer, and a training round count of 300.

In this study, the following indicators were used to evaluate the performance of the model: Precision (P), Recall (R), and Mean Average Precision (mAP). The calculation method for each indicator is shown in Equations (11)-(14):

$$P = \frac{TP}{TP + FP} \quad (11)$$

$$R = \frac{TP}{TP + FN} \quad (12)$$

$$AP = \int_0^1 PRdr \quad (13)$$

$$mAP = \frac{1}{N} \sum_{i=0}^n AP_i. \quad (14)$$

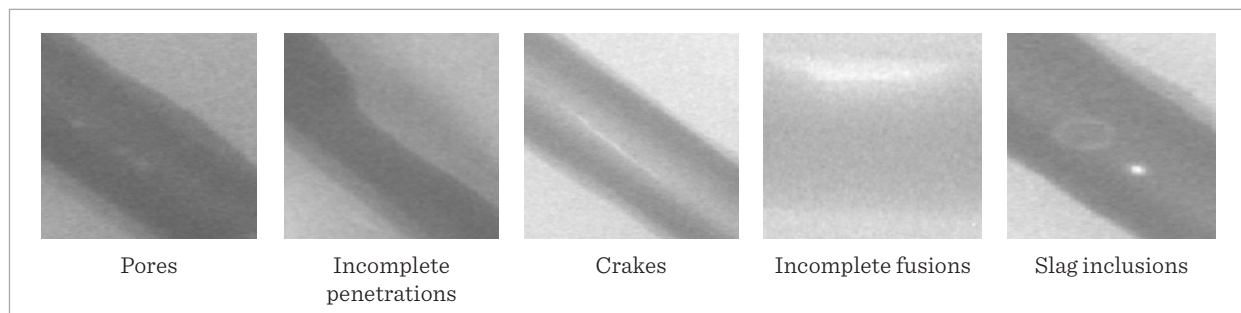
Among them, are the number of correctly predicted positive samples, the number of incorrectly predicted negative samples, and the number of incorrectly predicted positive samples. To study the balance between lightweight and model recognition accuracy, floating-point operations (FLOPs) are introduced. FLOPs refer to the total number of floating-point operations performed by an algorithm or model in the fields of computer science and numerical computing. This indicator is usually used to measure the computational complexity of an algorithm or model, rather than the specific runtime. By comparing the FLOPs of different models, it is possible to preliminarily evaluate their differences in computation. Fewer FLOPs may mean that the model is lighter and more suitable for running in resource-constrained environments.

4.2. Experimental Analysis

This article takes YOLOv8n as the baseline and introduces the VanillaNet module in the backbone network and bottleneck network to reduce the overall complexity of the model. At the same time, the BRA module and CARAFE upsampling operator are introduced in the bottleneck network to improve the recognition ability of small defects and enhance the expression ability of output features, respectively, to further improve the detection and recognition accuracy of the model. To verify the effectiveness of the baseline model improvement in this article, ablation experiments were conducted on the steel pipe weld defect dataset. By gradually adding optimization

Figure 5

Common five types of pipeline weld defect detection diagrams



modules to the baseline model, performance indicators before and after ablation were compared, and the effects of model parameter quantity, detection accuracy, and detection speed on model variation were analyzed. The contributions of each part of the model to pipeline weld defect detection and their interrelationships were compared.

According to the results of the ablation experiment, as shown in Table 1, it can be analyzed:

- 1 After adding the BRA structure to the bottleneck network, the computational complexity of the model decreased by 2.6 GFLOPs compared to the baseline, and the improvement in model inference speed was particularly significant, increasing from 232 to 333 at the baseline, an increase of 101. The model not only selects the target more accurately overall but also obtains the receptive field content of local areas more accurately. Significantly improved the detection accuracy of defects such as pores, cracks, and slag inclusions. This confirms that the BRA attention mechanism based on double-layer routing has a more accurate ability to select receptive fields.
- 2 After introducing the VanillaNet module into the backbone and bottleneck networks, the parameter count decreased from baseline 3.02M to 1.32M, a decrease of 1.7M. The computational load decreased from baseline 8.2GFLOPs to 5.1GFLOPs, a decrease of 3.1GFLOPs, and FPS improved by 86 compared to baseline. VanillaNet uses a continuous convolution pooling structure to extract features, avoiding branch structures and reducing a large amount of computation. Therefore, using lightweight VanillaNet modules as feature extraction can effectively reduce model complexity and improve inference speed.
- 3 After introducing the CARAFE upsampling module in the bottleneck network, the mAP of the model increased from 84.96% of the baseline to 86.14%, an improvement of 1.18%. The detection accuracy of defects such as porosity, incomplete penetration, and cracks has been improved, with cracks having the highest detection accuracy, reaching 88.8%. The number of parameters and computation increased by 0.13M and 0.6GFLOPs respectively compared to the baseline, while FPS de-

Table 1

Results of the Ablation Experiment

Model	BRA	VanillaNet	CARAFE	pores	Incomplete penetrations	cracks	Incomplete fusions	Slag inclusions	mAP (%)	Params (M)	GFLOPs	FPS
Base-Line+	-	-	-	82.8	83.2	86	88.4	84.4	84.96	3.02	8.2	236
Base-Line+	√			87.2	83.6	88.4	88.6	86.4	86.84	4.64	5.8	342
Base-Line+		√		81.4	81	87.6	82.8	84	83.36	1.32	5.1	322
Base-Line+			√	83.6	84.6	88.8	86.5	87.2	86.14	3.15	8.8	222
Base-Line+		√	√	81.2	83.8	86.6	87.6	85.5	84.94	1.45	6.0	275
Base-Line+	√	√		86.6	83.5	88.8	83.9	88.6	86.28	1.42	5.6	282
Base-Line+	√	√	√	87.8	86.2	90.2	88.2	87.5	87.98	1.56	6.2	275

creased by 14. Verified that the CARAFE operator can achieve upsampling by learning the correlation between pixels in the neighborhood, thereby capturing richer contextual information and facilitating the reconstruction of detailed features. Although it slightly increased the computational complexity, it significantly improved the detection accuracy of the model.

- 4 After introducing both the VanillaNet and BRA modules simultaneously, the model's parameter count and computational complexity were reduced by 1.6M and 2.6GFLOPs compared to the baseline, FPS was improved by 46, mAP was improved by 1.32%, and defect detection accuracy was improved; After introducing both the VanillaNet module and the CARAFE upsampling module simultaneously, the mAP of the model is consistent with the baseline. The number of parameters and computational complexity of the model decreased by 1.57M and 2.2GFLOPs respectively compared to the baseline, while FPS increased by 39.
- 5 After introducing the BRA module, VanillaNet module, and CARAFE upsampling module simultaneously, the YOLOv8n-BVS model achieved a maximum mAP of 87.98%, while the parameter and computational complexity were only 51.6% and 75.6% of the baseline, and the FPS increased by 39 compared to the baseline. The experiment has confirmed that the model proposed in this article has high recognition accuracy and faster recognition speed in pipeline weld defect detection and recognition tasks, promoting the industrial deployment of intelligent online detection and recognition of weld defects.

To further verify the recognition ability of the YOLOv8n-BVS model for small defects, an experimental comparison was made between the YOLOv8n model and the YOLOv8n-BVS model in this paper to identify the attention heatmap of small defect areas in pipeline welds, as shown in Figure 6. The experiment selected continuous micro pore defects and small cracks defects. The baseline model focused more on global targets when identifying these two types of defects and could not extract local features, In the case of larger computational complexity, the YOLOv8n-BVS model is unable to effectively identify small defect targets. However, it can quickly locate the key parts of the target, determine the position and

boundary of the target area, and efficiently complete the task of identifying pipeline weld defects.

5. Conclusion

In the field of pipeline weld defect detection, the limited computing power of terminal devices often makes it challenging to deploy deep learning models for real-time online detection and recognition of weld defects. This article proposes the lightweight YOLOv8n-BVS pipeline weld defect detection algorithm, which incorporates the BRA network structure, VanillaNet module, and CARAFE upsampling module. The model improves the ability to select targets and detect subtle defects more accurately. Although the improvements in model inference speed and computational complexity are incremental, the model still achieves a notable enhancement in efficiency. By reducing the number of parameters and computational requirements, the FPS increased, and the computational resources needed for inference were reduced compared to the baseline model. In practical production environments, the model achieved a mean average precision (mAP) of 87.98% on the pipeline weld defect dataset, with model parameters and computational complexity at only 51.6% and 75.6% of the baseline, respectively. The YOLOv8n-BVS model requires fewer computational resources to maintain high detection accuracy. With its precise defect detection, efficient performance, and strong applicability, it offers a valuable solution for real-time pipeline weld defect detection, meeting the demands of online monitoring in industrial settings.

Data availability statement

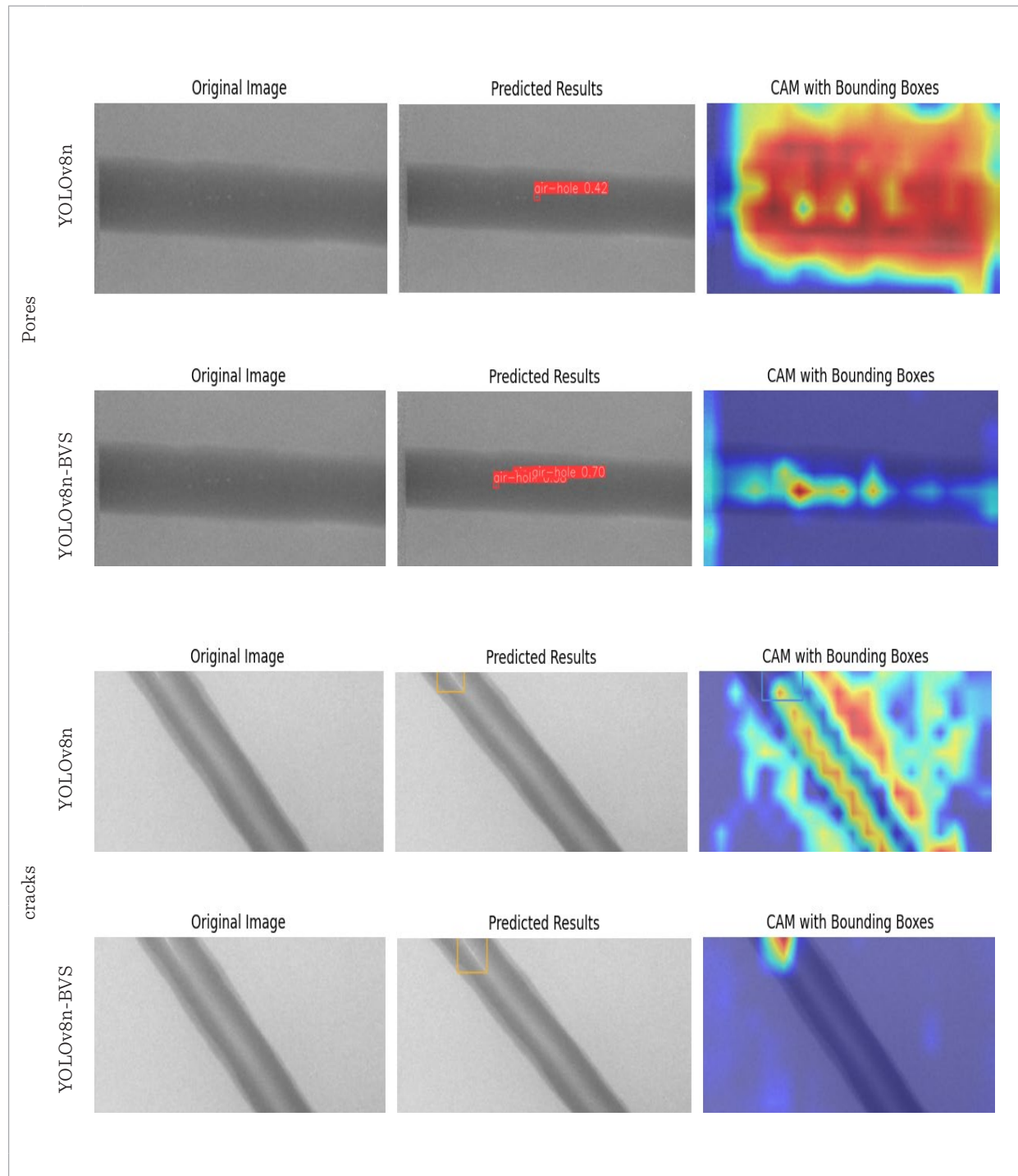
The data cannot be made publicly available upon publication because no suitable repository exists for hosting data in this field of study. The data that support the findings of this study are available upon reasonable request from the authors.

Funding

This research was funded by the Guiding Project of the Science and Technology Research Program of the Hubei Provincial Department of Education (Grant: B2023538).

Figure 6

Comparison between the YOLOv8n model and the YOLOv8n-BVS model in this paper for attention thermography of identifying small defects in pipeline welds



References

1. Amarnath, M., Sudharshan, N., Srinivas, P. Automatic Detection of Defects in Welding Using Deep Learning-A Systematic Review. *Materials Today: Proceedings*, 2023. <https://doi.org/10.1016/j.matpr.2023.03.268>
2. Chen, H., Wang, Y., Guo, J. VanillaNet: The Power of Minimalism in Deep Learning. *Advances in Neural Information Processing Systems*, 2024, 36. <https://doi.org/10.48550/arXiv.2305.12972>
3. Chen, P., Li, R., Fu, K. Mechanical Systems and Signal Processing, 2024, 206, 110919. <https://doi.org/10.1016/j.ymsp.2023.110919>
4. Gao, B., Zhao, H., Miao, X. Quality Assessment Algorithm of X-Ray Images in Overall Girth Welds Based on Deep Neural Network. *Journal of Pipeline Systems Engineering and Practice*, 2023, 14(1), 04022073. <https://doi.org/10.1061/JPSEA2.PSENG-1350>
5. Golodov, V. A., Maltseva, A. A. Approach to Weld Segmentation and Defect Classification in Radiographic Images of Pipe Welds. *NDT & E International*, 2022, 127, 102597. <https://doi.org/10.1016/j.ndteint.2021.102597>
6. Ji, C., Wang, H., Li, H. Defects Detection in Weld Joints Based on Visual Attention and Deep Learning. *NDT & E International*, 2023, 133, 102764. <https://doi.org/10.1016/j.ndteint.2022.102764>
7. Kenzhekhan, A., Bakytzhanova, A., Omirbayev, S. Design and Development of an In-Pipe Mobile Robot for Pipeline Inspection with AI Defect Detection System. 2023 23rd International Conference on Control, Automation and Systems (ICCAS), IEEE, 2023, 579-584. <https://doi.org/10.23919/ICCAS59377.2023.10316817>
8. Kumar, D., Fang, C., Zheng, Y. Semi-Supervised Transfer Learning-Based Automatic Weld Defect Detection and Visual Inspection. *Engineering Structures*, 2023, 292, 116580. <https://doi.org/10.1016/j.engstruct.2023.116580>
9. Li, L., Ren, J., Wang, P. Defect Detection Method for High-Resolution Weld Based on Wandering Gaussian and Multi-Feature Enhancement Fusion. *Mechanical Systems and Signal Processing*, 2023, 199, 110484. <https://doi.org/10.1016/j.ymsp.2023.110484>
10. Liu, M., Chen, Y., Xie, J. LF-YOLO: A Lighter and Faster YOLO for Weld Defect Detection of X-Ray Image. *IEEE Sensors Journal*, 2023, 23(7), 7430-7439. <https://doi.org/10.1109/JSEN.2023.3247006>
11. Purnomo, T. W., Danitasari, F., Handoko, D. Weld Defect Detection and Classification Based on Deep Learning Method: A Review. *Jurnal Ilmu Komputer dan Informatika*, 2023, 16(1), 77-87. <https://doi.org/10.21609/jiki.v16i1.1147>
12. Tan, M., Pang, R., Le, Q. V. EfficientDet: Scalable and Efficient Object Detection. *Proceedings of the IEEE/CVF Conference on Computer Vision and Pattern Recognition*, 2020, 10781-10790. <https://doi.org/10.1109/CVPR42600.2020.01079>
13. Tripicchio, P., Camacho-Gonzalez, G., D'Avella, S. Welding Defect Detection: Coping with Artifacts in the Production Line. *The International Journal of Advanced Manufacturing Technology*, 2020, 111(5), 1659-1669. <https://doi.org/10.1007/s00170-020-06146-4>
14. Wang, G. Q., Zhang, C. Z., Chen, M. S. YOLO-MSAPF: Multi-Scale Alignment Fusion with Parallel Feature Filtering Model for High-Accuracy Weld Defect Detection. *IEEE Transactions on Instrumentation and Measurement*, 2023. <https://doi.org/10.1109/TIM.2023.3302372>
15. Wang, X., Yu, X. Understanding the Effect of Transfer Learning on the Automatic Welding Defect Detection. *NDT & E International*, 2023, 134, 102784. <https://doi.org/10.1016/j.ndteint.2022.102784>
16. Wang, T., Li, Y., Zhai, Y. A Sewer Pipeline Defect Detection Method Based on Improved YOLOv5. *Processes*, 2023, 11(8), 2508. <https://doi.org/10.3390/pr11082508>
17. Xu, L., Dong, S., Wei, H. Intelligent Identification of Girth Welds Defects in Pipelines Using Neural Networks with Attention Modules. *Engineering Applications of Artificial Intelligence*, 2024, 127, 107295. <https://doi.org/10.1016/j.engappai.2023.107295>
18. Xu, X., and Li, X. Research on Surface Defect Detection Algorithm of Pipeline Weld Based on YOLOv7. *Scientific Reports*, 2024, 14(1), 1881. <https://doi.org/10.1038/s41598-024-52451-3>
19. Xu, H., Yan, Z. H., Ji, B. W. Defect Detection in Welding Radiographic Images Based on Semantic Segmentation Methods. *Measurement*, 2022, 188, 110569. <https://doi.org/10.1016/j.measurement.2021.110569>
20. Yuksel, V., Tetik, Y. E., Basturk, M. O. A Novel Cascaded Deep Learning Model for the Detection and Quantification of Defects in Pipelines via Magnetic Flux Leakage Signals. *IEEE Transactions on Instrumentation and Measurement*, 2023. <https://doi.org/10.1109/TIM.2023.3272377>

21. Yahaghi, E., Movafeghi, A., Mirzapour, M. Welded Pipe Defect Detection Enhancement Using Regularized Kernel Estimation-Based Image Processing in Radiographic Testing. *Russian Journal of Nondestructive Testing*, 2022, 58(8), 760-767. <https://doi.org/10.1134/S1061830922080046>
22. Zeyu, Y., Qi, M., Hongqiang, Y. Defect Identification Method for Ultrasonic Inspection of Pipeline Welds Based on Cross-Modal Zero-Shot Learning. *Measurement Science and Technology*, 2023, 35(2), 025009. <https://doi.org/10.1088/1361-6501/ad0613>
23. Zhang, X., Feng, J., Lu, S. FMD-Framework: A Size Estimation Method for Pipeline Defects in Weld-Affected Zones. *IEEE Transactions on Instrumentation and Measurement*, 2023, 72, 1-11. <https://doi.org/10.1109/TIM.2023.3250239>



This article is an Open Access article distributed under the terms and conditions of the Creative Commons Attribution 4.0 (CC BY 4.0) License (<http://creativecommons.org/licenses/by/4.0/>).